Potentialities of lidar-type single-sided optical tomography of tissues

Ljuan L. Gurdev*, Tanja N. Dreischuh, and Dimitar V. Stoyanov
Institute of Electronics, Bulgarian Academy of Sciences
72 Tzarigradsko shosse blvd., 1784 Sofia, Bulgaria

ABSTRACT

The potentialities are investigated of a single-sided optical tomography approach based on lidar principle. Concretely, the informative depth of sensing is estimated that outlines the underside area in the probed object where one could reveal inhomogeneities with some desirable contrast. The sensing radiation is supposed to consist of picosecond laser pulses with pulse repetition rate of ~ 10 MHz and optimum wavelength of 800 nm. The maximum permissible skin exposure is considered as determinant. The longitudinal and the transversal resolution intervals are chosen to be 2 mm and 3 mm (or 1 cm), respectively. It is shown that, under the above described conditions, inhomogeneities with contrast 1-10 % would be detected at depths of 1 to 4 cm, depending mainly on the values of the attenuation coefficient chosen here to vary correspondingly from 1.4 mm^{-1} to 0.4 mm^{-1}.

Keywords: optical tomography, lidar, tissue, breast tissue.

1. INTRODUCTION AND FORMULATION OF THE PROBLEM

Optical tomography is an important hopeful investigation area that is expected to provide effective non-invasive methods and instruments for early diagnosis of serious human tissue diseases. The main advantage here is the absence of risks of ionizing irradiation. There are many variants of optical tomography being developed at present that are aimed mainly at the determination of 2D images of small objects hidden in turbid media.[1-7] Recently we developed a double-sided tomographic approach based on lidar principle[8] consisting in illuminating the investigated object by narrow-beam pulsed laser radiation from both the opposite sides along the line of sight (LOS). Then, after processing both the corresponding recorded time-to-range resolved backscattering (lidar) profiles, one can determine unambiguously the LOS distribution within the object of the backscattering and extinction (attenuation) coefficients. A 3D distribution of these coefficients is obtainable by a lateral parallel scan or a set of parallel sensing beams. The achievable range resolution scale is conditioned here by the larger of the sensing pulse length and the sampling interval. The transversal sensing resolution is conditioned by the cross section of the sensing laser beam. We should especially note that the double-sided approach[8] is intended for investigating translucent media with prevailing single-scattering effects. It is not applicable at all to turbid media with relatively large sizes, because of strong attenuation with depth of the lidar signal, and restricted permissible irradiation dose. Such media may be probed however from any suitable single side, to some depth from where the signal is sufficiently strong and informative. Similar lidar-type single-sided optical tomography (illustrated in Fig.1) would have some favorable properties making it advantageous over other known optical tomography techniques. First, the time-to-range resolved signal detection ensures automatically the location of attenuation and backscattering inhomogeneities within the object. Second, the lidar equation, describing the relation between the detected signal and the material characteristics, is unambiguously and independently solvable, for each LOS, with respect to the extinction and backscattering profiles. And third, the backward signal detection ensures lower (compared to the transmission-based methods) multiple scattering noise level. As a whole, the lidar-type sensing is characterized by simple, clear and currently controllable measurement and data-processing procedures. Besides, the results to be obtained about the 3D spatial distribution of the extinction and backscattering coefficients within an object, represent a profound-enough information about the object status.

Because of the above-mentioned favorable features, it is worth estimating the potentialities of the lidar-type optical tomography of biological objects. Correspondingly, the main purpose of the present study is to estimate the basic characteristic of the potentialities of the method, the informative depth of sensing (IDS), depending on the measurement time and the detectable contrast required.

* E-mail: lugurdev@ie.bas.bg

14th International School on Quantum Electronics: Laser Physics and Applications,
edited by Peter A. Atanasov, Tanja N. Dreischuh, Sanka V. Gateva, Lubomir M. Kovachev,
Proc. of SPIE Vol. 6604, 66042I, (2007) 0277-786X/07/$15 doi: 10.1117/12.727718

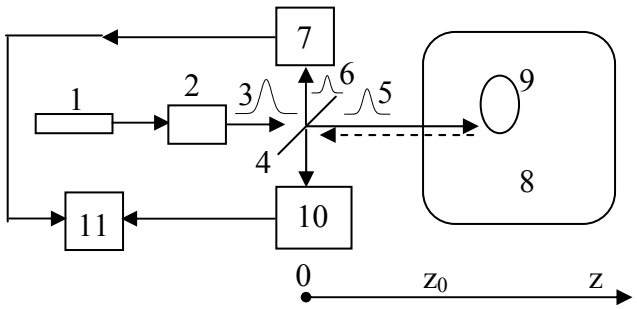

Fig.1. Illustration of lidar-type sensing of turbid objects: 1 is a pulsed laser source, 2 is beam-forming optics, 3 is an emitted light pulse, 4 is a beam splitter, 5 is a sensing light pulse, 6 is a reference light pulse, 7 is a block of receiving and detecting the reference light pulse and forming an electronic start pulse, 8 is the probed object, 9 is an ingredient inside the object, 10 is a system of receiving and detecting the backscattered radiation, 11 is a block of time-to-range resolved data acquisition and processing.

2. IDS AND PROBLEMS CONCERNING ITS ESTIMATION

IDS of a lidar[9] is the maximum depth within the probed object from where the signal is still sufficiently strong to be measured with the required accuracy that is usually characterized by the maximum relative measurement error. The relative error is in fact a measure of the detectable contrast. So, IDS itself outlines an underside area within the object where one could reliably detect and characterize important ingredients with some determinate contrast. To apply the lidar-type sensing approach to turbid media one should maximally restrict the contribution of the multiple-scattering background to the detected return radiation. Then, the selected single-backscattering return would be too feeble and detectable only by photon counting. The evaluation of the informative depth of lidar-type sensing is natural to be based on some relation like the lidar equation[10]. According to some recently obtained results[11] concerning pulsed-beam propagation and scattering in turbid media with sharply forward directed Henyey-Greenstein indicatrix, such a relation is

$$N_T(z,\Delta z) = \Omega\eta N_{ET}\Delta z\beta(z)\exp\left\{-2\int_{z_0}^{z}\alpha(z')dz'\right\} \quad , \tag{1}$$

where $N_T(z,\Delta z)$ is the mean number of signal photon counts accumulated for the exposure time T and resulting from detection of the signal photons backscattered within the region $[z, z+\Delta z]$ along the LOS, N_{ET} is the mean exposure dose (in photon number) deposited along the LOS for the period T, Ω is the solid angle of acceptance of the receiving system of the lidar, η is the photodetector quantum efficiency, Δz is the range resolution bin (pixel) along the LOS, $\beta(z)$ is the LOS profile of the volume backscattering coefficient (BSC), $\alpha(z)$ is the LOS profile of the linear attenuation coefficient, and z_0 is the LOS coordinate of the "entrance" into the investigated object. Eq.(1) is derived under the assumption that the object is irradiated by sufficiently short laser pulses (say, with 10-20 ps duration) ensuring a relatively high range resolution of about 1-3 mm. The LOS coordinate z of the scattering events is specified, during the signal detection procedure, according to the relation $z=ct/2$. The expression obtained of α is

$$\alpha(z) = \mu_a(z) + \mu_s'(z)/\{2[1+g(z)]^2\} \quad , \tag{2}$$

where (see e.g. in [12]) $\mu_a(z)$ is the volume absorption coefficient (AC), $\mu_s'(z)=\mu_s(z)[1-g(z)]$ is the reduced scattering coefficient (RSC), $g(z)$ is the scattering anisotropy factor (AF), and $\mu_s(z)$ is the total scattering coefficient (TSC). It is natural to assume that the realizations $\hat{N}_T(z,\Delta z)$ of the photon counts accumulated for the measurement period T have Poissonian statistics and, respectively, mean value $<\hat{N}_T(z,\Delta z)>= N_T(z,\Delta z)$ and variance $VarN_T(z,\Delta z) = <[\hat{N}_T(z,\Delta z) - N_T(z,\Delta z)]^2>= N_T(z,\Delta z)$; <.> denotes ensemble average. Then, the relative signal measurement error will be $\delta_r N_T = (Var\ N_T / N_T^2)^{1/2} = N_T^{-1/2}$. Thus, to achieve a required detectable minimum contrast δ_c (at a maximum admissible relative error $\delta_r N_T = \delta_c$) one should store up at least $N_{T\min} = \delta_c^{-2}$ photon counts. In a homogeneous medium the signal profile $N_T(z,\Delta z)$ is decreasing function of z. Therefore, at some depth $D = z_l - z_0$ in a probed homogeneous object [with $\alpha(z)=\alpha$=const and $\beta(z)=\beta$=const] the signal would drop to δ_c^{-2}, i.e., $N_T(z_l,\Delta z)=N_{T\min}$. At larger depths, when $z > z_l$, no inhomogeneities would be detected with the required contrast. For this reason D may be defined as the informative depth of sensing and considered as a basic potentiality characteristic. The expression of IDS is directly obtainable from Eq.(1) in the form

$$D = -0.5\ \alpha^{-1}\ln\{N_{T\min}/(Q\beta)\} \ , \tag{3}$$

where $Q=\Omega\eta N_{ET}\Delta z$.

A major factor restricting IDS in tissues is the maximum permissible exposure to laser radiation. We shall further deal with the maximum permissible skin exposure (MPSE) to optimum[13-15] picosecond pulsed radiation with wavelength λ=800 nm and typical pulse repetition rate from 10 to 80 MHz. Based on the contemporary standards (e.g., BS EN 60825:1994 and ANSI Z 136:1986) for such radiation the relation between MPSE and the exposure duration T [s] is

$$\mathrm{MPSE} = 1.1\mathrm{x}10^{0.002(10^9\lambda - 700)}\, T^{1/4} \ \ [\mathrm{J.cm^{-2}}] \ , \tag{4}$$

For λ=8x10^{-7} m we obtain $$\mathrm{MPSE} = 1.76\ T^{1/4}\ [\mathrm{J.cm^{-2}}] \ , \tag{5}$$

from where one can account that for T = 600 s (10 min) MPSE is 8.71 J.cm^{-2}.

The dispersion of the existing data about RSC, g, and AC of tissues, including breast tissue, is too large. In practice, there are no data about BSC. There are various works, where μ_a, μ_s', and g of different tissues, for different wavelengths λ, are determined **in vitro**[16,17] or **in vivo**[7,18,19] (or by using fantoms[4,20]), in direct[16,17] or indirect[4,18-20] ways. Some of the results obtained are given in Table 1. It is seen that the data for μ_s' of healthy or diseased breast tissue, obtained by different approaches in vivo or in vitro, are about 1 mm^{-1} on the average, with a relative variation of about 20-50 %. A drastically differing result (4-12 mm^{-1}) is implied on the basis of the data, obtained in vitro in Ref.16. The values obtained in vivo for the AC are 2-3 orders of magnitude smaller. The results for AC obtained in vitro are one order of magnitude larger than ones obtained in vivo. The existing data about the anisotropy factor g of liver, lung uterus, and rat liver vary from 0.7 to 0.96.[16,21] On this basis one may use for the estimation to be conducted an average value of g=0.85. There are no data about β, but one can meet some experimental results about the angular (Henyey-Greenstein) scattering distribution from different tissues such as liver, lung, and uterus.[16] If we assume that the scattering phase function is of Henyey-Greenstein type, for the BSC we obtain

$$\beta = \mu_s (1-g)/[4\pi(1+g)^2] = \mu_s'/[4\pi(1+g)^2] \ . \tag{6a}$$

We shall further neglect μ_a in Eq.(2) and assume that

$$\alpha = \mu_s'/[2(1+g)^2] \ . \tag{6b}$$

Then we have

$$\alpha = 2\ \pi\beta. \tag{6c}$$

For μ_s' = 1 mm^{-1} and g=0.85 we obtain that $\alpha \cong 0.15$ mm^{-1}. This value seems too small, but it is as reliable as the data for μ_s' are. In the following estimation it will be considered as a lower limit. The other values employed of α are larger and vary from 0.4 mm^{-1} to 1.4 mm^{-1} with a step $\Delta\alpha$ = 0.2 mm^{-1}.

Table. 1. Optical parameters of tissues.

Tissue	**Sample**	**Method**	**Wavelength** (nm)	**AC** μ_a (mm^{-1})	**RSC** μ_s' (mm^{-1})	**AF** g	**Refe-rence**
healthy breast healthy breast breast Ca	in vivo in vitro in vitro		800 700-900 700-900	0.002-0.003 0.022-0.075 0.045-0.050	0.72-1.22 0.53-1.42 0.89-1.18		14
healthy breast liver, lung uterus	in vitro	measurement of thin section of material	635	< 0.02	4-12	~ 0.7	16
healthy breast healthy breast breast Ca breast Ca	in vivo in vivo in vivo in vivo	noninvasive optical method including frequency domain optical mammography and diffusion theory	690 825 690 825	0.0030 0.0040 0.0084 0.0085	1.20 1.40 1.50 1.27		7
healthy breast breast Fa	in vivo in vivo	frequency domain approach	750 750	0.004 0.008	1.2-1.4-1.6 1.0		18
healthy breast	in vivo	frequency domain approach	785	0.0057-0.0063	1.0		19
rat liver	in vivo	measurements of integrated transmittance and reflectance	800	0.57	0.58	0.94	21

3. PREMISED PARAMETERS AND RESULTS OBTAINED FOR IDS

The IDS D (for breast tissue implied) is estimated, assuming the following values of the parameters of importance (see also Eq.1): η=0.2, Δz=2 mm, λ=800 nm, T=600 s, and g=0.85; Ω=0.0314 sr at beam diameter of 3 mm permitting 0.615 J fluence, i.e., $N_{ET} \cong 2.5\text{x}10^{18}$ photons (Case a); Ω=0.1256 sr at beam diameter of 11 mm permitting 8.71 J fluence, i.e., $N_{ET} \cong 3.5\text{x}10^{19}$ photons (Case b); and required measurement accuracy $\delta_c\,(=N_{T\,\min}^{-1/2})$ of 1%, 3%, and 10% corresponding to minimum stored photons per pixel $N_{T\min}$=10^4, 10^3 and 10^2. The above premised parameters, together with the varying values of α and the final results for D, are given in Table 2. The results for D are additionally illustrated in Fig.2. It is seen that, as one may expect, the main factor [taking part in the exponent in Eq.(1)] determining the value of D is the attenuation coefficient α; the influence of the pre-exponential factors Ω, η, N_{ET}, and Δz, as well as of δ_c, is weaker. The main result from the estimation performed is that the lidar type sensing of (breast) tissue would enable one to detect and image 1-10% contrast abnormalities to depths of 1-3 cm and even 4 cm.

Table. 2. Estimated values of IDS, depending on the attenuation coefficient α, under different experimental conditions and requirements.

Informative depth of sensing *D* (mm)						
	Case (a)			Case (b)		
α (mm^{-1})	δ_c = 1 %	δ_c = 3 %	δ_c = 10 %	δ_c = 1 %	δ_c = 3 %	δ_c = 10 %
1.40	9.74	10.56	11.38	11.17	11.99	12.82
1.20	11.26	12.21	13.17	12.93	13.88	14.84
1.00	13.47	14.62	15.77	15.48	16.63	17.78
0.80	16.70	18.14	19.57	19.21	20.65	22.09
0.60	22.06	23.99	25.91	25.43	27.35	29.27
0.40	32.53	35.40	38.28	37.56	40.44	43.31
0.15	83.51	91.19	98.87	96.93	104.61	112.29

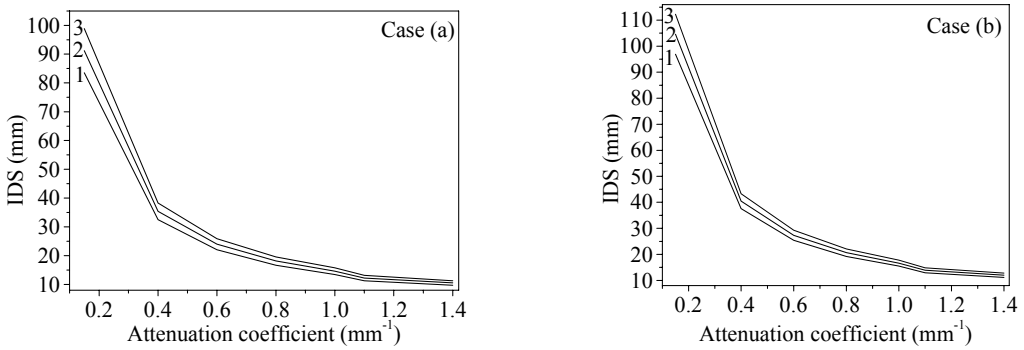

Fig.2. Estimated values of the informative depth of sensing D versus the attenuation coefficient α, at a required contrast of 1% (1), 3% (2), and 10% (3).

4. CONCLUSION

The investigations performed in the work show that, according to the available now data about the absorption and reduced-scattering coefficients and the scattering phase function of tissues as well as about the maximum permissible exposure to pulsed radiation of 800 nm wavelength, the lidar-type optical sensing of (breast) tissues would be effective to depths of 1-3 cm and even 4 cm, depending on the value of the attenuation coefficient α, at a detectable contrast of 1-10%. Certainly, the lidar type sensing could (and should) be employed for providing reliable data for α and β, and thus for indirectly checking the corresponding results for μ_a, μ_s', and g obtained by other methods.

Let us note at last that a realization of lidar-type optical sensing and tomography of tissues would require high PRR trains of short-enough (say, of 10 to 20 ps duration) sensing pulses and extremely fast (say again, of 10 to 20 ps temporal resolution) signal-photon detectors and electronic methods and instruments for signal processing (e.g., Ref. 22). In this way one would achieve an imaging resolution of the order of several (one to three) millimeters.

ACKNOWLEDGEMENTS

This work was supported in part by the Bulgarian National Science Fund under grant F-1511.

REFERENCES

1. M.R. Hee et al., "Femtosecond transillumination optical coherence tomography," *Opt. Lett.* 18(12), 950-952 (1993).
2. H.P. Chiang, "Reflective tomography in random scattering media by continuous-wave broadband electronic holography," *Opt. Eng.* 35(2), 575-578 (1996).
3. J.A. Moon, R. Mahon, M.D. Duncan, and J. Reintjes, "Three dimensional reflective image reconstruction through a scattering medium based on time gated Raman amplification," *Opt. Lett.* 19(16), 1234-1236 (1994).
4. J.C. Hebden, D.J. Hall, M. Firbank, and D.T. Delphy, "Time-resolved optical imaging of a solid tissue-equivalent phantom," *Appl. Opt*. 34(34) 8038-8047 (1995).
5. F.E.W. Schmidt, M.E. Fry, E.M.C. Hillman, J.C. Hebden, and D.T. Delphy, "A 32-channel time-resolved instrument for medical optical tomography," *Rev. Sci. Instrum*. 71(1), 256-265 (2000).
6. J.B. Fishkin, O. Coquoz, E.R. Anderson, M. Brenner, and B.J. Thomberg, "Frequency-domain photon migration measurements of normal and malignant tissue optical properties in a human subject," *Appl. Opt.* 36(1),10-20 (1997).
7. S. Fantiny et al., "Assessment of the size, position and optical properties of breast tumors in vivo by noninvasive optical methods," *Appl. Opt*. 37(10), 1982-1989 (1998).
8. L.L. Gurdev, T.N. Dreischuh and D.V Stoyanov, "Pulse backscattering tomography based on lidar principle," *Opt. Commun.* 151(6), 339-352 (1998).
9. L.L. Gurdev, D.V Stoyanov, T.N. Dreischuh, Ch.Protochristov, and O. Vankov, "Gamma-ray backscattering tomography approach based on the lidar principle", *IEEE Trans. Nucl. Sci.* 54, accepted (2007).
10. V. A. Kovalev, W.E. Eichinger, *Elastic Lidar: Theory, Practice, and Analysis Methods*, Wiley, New York, 2004.
11. L.L. Gurdev, Recently obtained, still unpublished results.
12. A. Ishimaru, "Wave propagation and scattering in random media. Volume 1: Single scattering and transport theory", Academic Press, New York, 1978.
13. S. Fantini E.L. Heffer, H. Siebold, and O. Schueltz, "Using near-infrared light to detect breast cancer," *Optics & Photonics News*, November 2003, pp. 24-29.
14. F. E.W. Schmidt, "Development of a time-resolved optical tomography system for neonatal brain imaging," PhD Thesis, University of London, 1999.
15. T. D. Yates, "Time-resolved optical tomography for the detection and specification of breast disease," PhD Thesis, University of London, 2005.
16. R. Marchesini at al., "Extinction and absorption coefficients and scattering phase functions of human tissues in vitro," *Appl. Opt.* 28(12), 2318-2324 (1989).
17. B.B. Das et al., "Spectral optical-density measurements of small particles and breast tissue," *Appl. Opt.* 32(4), 549-583 (1993).
18. T.O. McBride et al., "Initial studies of in vivo absorbing and scattering heterogeneity in near-infrared tomographic breast imaging," *Opt. Lett*. 26(11), 822-824 (2001).
19. S.Jiang et al., "In vivo near-infrared spectral detection of pressure-induced changes in breast tissue," *Opt. Lett.* 28(14), 1212-1214 (2003).
20. A. Pifferi et al., "Performance assessment of photon migration instruments: the MEDPHOT protocol", *Appl. Opt*. 44(11), 2104-2114 (2005).
21. P. Parsa, S. Jacques, and N. Nishioka, "Optical properties of rat liver between 350 and 2200 nm," *Appl. Opt*. 28(12), 2325-2330 (1989).
22. D.V. Stoyanov, T.N. Dreischuh, O.I. Vankov, and L.L. Gurdev, " Measuring the shape of randomly arriving pulses shorter than the acquisition step," *Meas. Sci. Technol*. 15(10), 2361-2369 (2004).